Real-Time Classification of Bladder Events for Effective Diagnosis and Treatment of Urinary Incontinence

Robert Karam*, *Student Member, IEEE*, Dennis Bourbeau, Steve Majerus, *Member, IEEE*, Iryna Makovey, Howard B. Goldman, Margot S. Damaser, *Senior Member, IEEE*, and Swarup Bhunia, *Senior Member, IEEE*

***Abstract*—Diagnosis of lower urinary tract dysfunction with urodynamics has historically relied on data acquired from multiple sensors using nonphysiologically fast cystometric filling. In addition, state-of-the-art neuromodulation approaches to restore bladder function could benefit from a bladder sensor for closed-loop control, but a practical sensor and automated data analysis are not available. We have developed an algorithm for real-time bladder event detection based on a single *in situ* sensor, making it attractive for both extended ambulatory bladder monitoring and closed-loop control of stimulation systems for diagnosis and treatment of bladder overactivity. Using bladder pressure data acquired from 14 human subjects with neurogenic bladder, we developed context-aware thresholding, a novel, parameterized, user-tunable algorithmic framework capable of real-time classification of bladder events, such as detrusor contractions, from single-sensor bladder pressure data. We compare six event detection algorithms with both single-sensor and two-sensor systems using a metric termed Conditional Stimulation Score, which ranks algorithms based on projected stimulation efficacy and efficiency. We demonstrate that adaptive methods are more robust against day-to-day variations than static thresholding, improving sensitivity and specificity without parameter modifications. Relative to other methods, context-aware thresholding is fast, robust, highly accurate, noise-tolerant, and amenable to energy-efficient hardware implementation, which is important for mapping to an implant device.**

***Index Terms*—Closed-loop control, event detection algorithms, incontinence, overactive bladder, spinal cord injury, urinary dysfunction.**

Manuscript received December 2, 2014; accepted August 5, 2015. Date of publication August 18, 2015; date of current version March 17, 2016. This work was supported in part by Grant 1I01RX000443-01A2, Grant 1IK1RX000960-01A1, and Grant 1IO1RX000822-01A1 from the Rehabilitation Research and Development Service of the VA Office of Research and Development, as well as resources and the use of facilities at the Louis Stokes Cleveland VA Medical Center, Cleveland Clinic, and Case Western Reserve University. *Asterisk indicates corresponding author.*

*R. Karam is with the Department of Electrical Engineering and Computer Science, Case Western Reserve University, Cleveland, OH 44106 USA, and also with the Advanced Platform Technology Center, Louis Stokes Cleveland VA Medical Center, Cleveland, OH 44106 USA (e-mail: rak65@case.edu).

D. Bourbeau is with the Cleveland Functional Electrical Stimulation Center, Louis Stokes Cleveland VA Medical Center.

S. Majerus and S. Bhunia are with the Department of Electrical Engineering and Computer Science, Case Western Reserve University, and also with the Advanced Platform Technology Center, Louis Stokes Cleveland VA Medical Center.

I. Makovey and H. B. Goldman are with the Glickman Urological and Kidney Institute, Cleveland Clinic.

M. S. Damaser is with the Advanced Platform Technology Center, Louis Stokes Cleveland VA Medical Center, the Department of Biomedical Engineering, Lerner Research Institute, and the Glickman Urological and Kidney Institute, Cleveland Clinic.

Color versions of one or more of the figures in this paper are available online at http://ieeexplore.ieee.org.

Digital Object Identifier 10.1109/TBME.2015.2469604

I. Introduction

URINARY incontinence is a condition affecting 200 million people worldwide [1] and significantly reduces quality of life. Diagnosis of urinary incontinence can range from simple clinical evaluation based on history and a physical exam to more complex tests, such as a clinical urodynamics examination, to determine if the patient has stress urinary incontinence (SUI) or urgency urinary incontinence due to overactive bladder (OAB) or neurogenic detrusor overactivity [2]. During a clinical urodynamics test, the bladder is filled with saline at nonphysiologically high infusion rates for one or two cystometric fills. Two separate pressure sensors, one measuring vesical pressure via an intraurethral catheter, and the other measuring abdominal pressure via a rectal balloon catheter, are used to determine bladder activity. True detrusor pressure is calculated as the simultaneous difference between the abdominal pressure and the vesical pressure: $P_{\text{detrusor}} = P_{\text{vesical}} - P_{\text{abdominal}}$. The detrusor pressure is then used to distinguish between bladder contraction events and abdominal-induced artifacts caused by coughs, laughs, or changes in posture [3]. The nonphysiologically high infusion rates allow for reasonably short examination times, but may irritate the bladder and confound pressure data, and the small number of cystometric fills provides little data for diagnosis. Extended ambulatory urodynamics testing can provide more data collected at physiologically normal fill rates [4], [5]. However, this two-sensor system provides an inconvenient and uncomfortable solution for extended ambulatory urodynamics testing. An alternative method of measuring bladder activity over extended durations at natural fill rates would improve diagnosis.

For treatment of urinary dysfunctions, electrical stimulation has been shown to effectively inhibit unwanted bladder contractions in both spinal cord injury patients [6]–[9] and neurally intact patients [10]. The Interstim (Medtronic, Minneapolis, MN) is an implantable open-loop, continuous-stimulation neuromodulator that is currently FDA approved for use in humans to control sensations of urgency [11]. A similar approach using stimulation has been shown to be effective for individuals with neurogenic detrusor overactivity [12]. Open-loop stimulation of the genital nerve is not ideal because the neural pathways could become habituated to continuous stimulation of sensory nerves, potentially reducing the effectiveness of stimulation over time. Stimulation settings may need to be adjusted over time, typically by the clinician. In addition, individuals with neurogenic detrusor overactivity require feedback of bladder activity in the absence of sensation to determine when to empty their

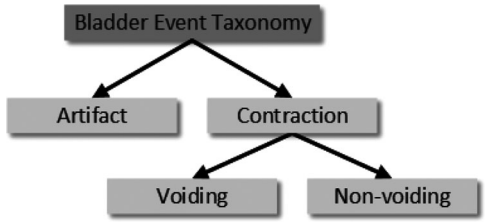

Fig. 1. Taxonomy of bladder events—artifacts, voiding, and nonvoiding contractions. Automatic detection of these events can aid in diagnosis and treatment of lower urinary tract dysfunction.

bladders, and those with sensation may not wish for stimulation to be continuously active for reasons of comfort. Closed-loop or conditional genital nerve stimulation has been shown to be as effective as open-loop stimulation for increasing bladder capacity [12], [13] while reducing power consumption and stimulation time [14], potentially reducing the cost of this treatment modality over time. However, such approaches require feedback to determine bladder activity for closed-loop control.

Both diagnosis and stimulation to improve urinary continence can greatly benefit from a system capable of categorizing bladder events in real time from a single pressure sensor. Generally, these events can be categorized into three types: bladder contraction resulting in voluntary voiding, bladder contraction without voluntary voiding, and abdominal artifact (see Fig. 1). Two approaches have been tested for chronic bladder monitoring. One approach measures bladder activity by decoding neural signals from the peripheral nerves of the lower urinary tract and has been used to estimate bladder volume or predict contractions [15]–[17]. However, the viability of this approach to determine bladder activity from nerve recordings is limited by the accuracy and stability of the decoding model and the mechanical stability of the neural interface. A second approach involves implantable sensors, which are capable of directly measuring bladder pressure [18]–[24]. This approach removes the need for an external catheter-based sensor and does not have the drawbacks of a neural recording approach. It remains to be shown if a single sensor is sufficient to identify bladder events or if a second abdominal sensor is required to distinguish these from abdominal and motion artifacts.

Previous work in event-driven or conditional stimulation has demonstrated the feasibility of detecting the onset of urinary bladder contractions from sensors implanted in the bladder wall using static thresholds [25], hereafter referred to as static detrusor thresholding [SDT, (1)], or a hybrid of static and adaptive thresholds [22], referred to as hybrid detrusor thresholding [HDT, (2)], summarized here:

$$\text{SDT} = \begin{cases} P_{\text{det}}(t) \geq T, & \text{Stimulation On} \\ P_{\text{det}}(t) < T, & \text{Stimulation Off} \end{cases} \quad (1)$$

$$\text{HDT} = \begin{cases} \text{avg}(30) + T \geq P_{det}(t), & \text{Stimulation On} \\ \text{avg}(30) + T < P_{det}(t), & \text{Stimulation Off} \end{cases} \quad (2)$$

If the detrusor pressure, P_{det}, at the current time, t, crosses a fixed threshold, T, then stimulation is turned ON under the assumption that a bladder contraction is occurring. The HDT algorithm adds a moving average of the previous 30 s, $\text{avg}(30)$, to account for drift. Because these algorithms identify a bladder contraction by pressure exceeding a threshold value, they are prone to administer stimulation at inappropriate times, such as when an individual coughs. If these algorithms overstimulate, then more power is consumed than necessary, the risk of habituation to stimulation is increased, and the user may be uncomfortable with stimulation at inappropriate times. To avoid false positives, a second sensor is required, but frequent resetting of the threshold may still be necessary.

This paper presents a context-aware thresholding (CAT) algorithm, which is a novel, tunable, wavelet-based adaptive algorithmic framework for rapid, accurate, and automatic detection of bladder events and rejection of artifacts without using a second, separate sensor. This algorithm has applications in both real-time and offline processing of single-sensor bladder pressure signals, or as a stimulation trigger in a closed-loop system. The event detection algorithm is amenable to efficient hardware implementation, which is important for mapping it inside an implant unit. We have developed an automated method for tuning our system to an individual patient using a set of operational parameters, thus maximizing the efficacy and efficiency through the use of a novel conditional stimulation scoring function. This system was validated using a set of prerecorded data from human subjects with neurogenic bladder in an emulated real-time environment.

II. Methods

The primary objective of our algorithm was to detect and identify bladder events, including contractions and stress events, without requiring a second sensor. The system requirements included amenability to efficient hardware implementation and the ability to maintain a high level of accuracy despite artifacts and other sources of physiological or sensor noise [26] and take into account the potential variation in the patient population, changes in patient physiology over time, or hardware issues, such as loss of sensitivity or sensor drift. The system also needed to be reprogrammable and tunable to an individual.

A. Vesical Pressure Signal Processing

The basic algorithm structure includes three stages: initial filtering, wavelet transform, and adaptive thresholding (see Fig. 2). The signal is initially filtered using an exponential moving average (EMA) [27], with a low-pass cutoff frequency of 0.01 Hz. EMA filtering is chosen because it allows the system to operate in an almost predictive manner by assuming that repeated spikes in pressure can potentially result in a true bladder contraction. For a hardware implementation, the computation is inexpensive, requiring very few operations and a single unit of delay, enabling real-time operation. Furthermore, by filtering close to DC, changes in pressure are effectively limited to those caused by passive stretching of the bladder. Contractions, which occur at higher frequencies, are sustained and, while slightly attenuated, remain present in the output. The output of the EMA is then processed by applying a multilevel discrete wavelet transform (DWT). We chose the Daubechies 4 wavelet as the basis

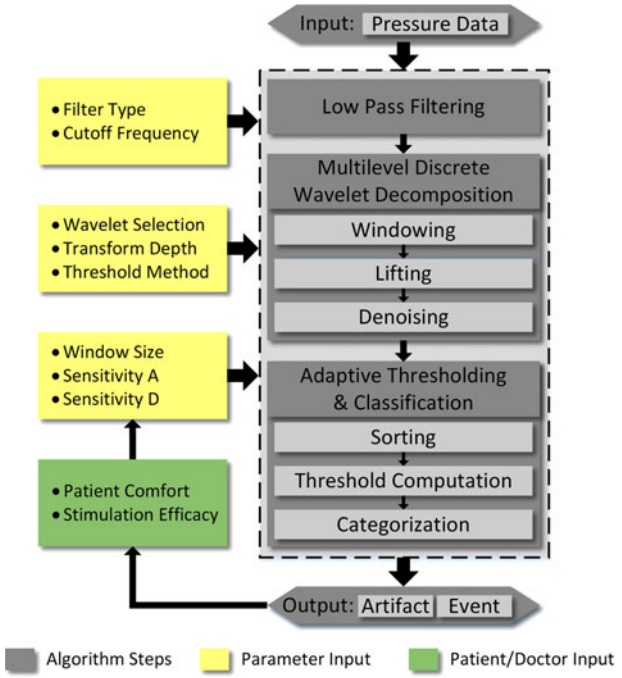

Fig. 2. Algorithm flow, with feedback. Low-pass filtering, wavelet transform, and adaptive thresholding are used to categorize contraction events and artifacts. Patient comfort and stimulation efficacy are not evaluated by the algorithm, but can be considered when adjusting parameter values.

function for use in the algorithm. This wavelet was chosen for its performance at extracting frequencies of interest for this application and its ease of implementation. Furthermore, the wavelets are constructed to minimize the number of filter coefficients required to approximate a given signal [28], reducing the computational burden on hardware implementation.

In clinical urodynamics, the effects of artifacts are negligible as patient motion and activity level are controlled, and a global threshold can work well for detecting bladder contractions. However, for ambulatory urodynamics without an abdominal reference sensor, a fixed threshold is vulnerable to patient movement and sensor drift. Thus, an adaptive threshold, which considers local trends in the data, may be more robust in a real-world ambulatory setting. We investigated two statistical methods of adaptive thresholding, which consider either the mean and standard deviation or the quantiles within a given window size.

Using standard-deviation-based thresholding, the algorithm labels a contraction when the approximation of the vesical pressure rises two standard deviations above the window mean. Similarly, artifacts are considered to occur when the detail coefficients, or outputs from the high-pass filters, rise by the same amount. At this stage, the original signal is heavily processed. Therefore, any residual artifacts will cause spikes in the detail coefficients, enabling detection. Since the bladder pressure approximation does not change significantly between subsequent windows, the mean need not be recomputed for each sample, providing a tradeoff between power savings and accuracy in hardware implementation.

Using the quantile-based adaptive thresholding, the values in the window are sorted by rank order. Samples in either the approximation or detail coefficients exceeding a threshold percentile are considered bladder events or artifacts, where the threshold percentile may be adjusted by the physician. Since the list remains partially sorted, new samples can be rapidly inserted into the list. Furthermore, separate significance threshold values for approximation and detail coefficients allow algorithm tuning based on the desired detection and false positive rates.

B. Algorithm Optimization and Output

The ability to optimize algorithm performance for a specific user is crucial to the successful implementation of the framework. To enable user-specific optimization, we introduced a set of tunable input parameters into the system. To provide this level of flexibility, the tunable parameters included 1) sample buffer length, 2) approximation coefficient sensitivity, and 3) detail coefficient sensitivity. The sample buffer length refers to the time in seconds of history to retain, while the approximation and detail coefficient sensitivity refer to the percentile required for a new input value to be classified as the start of a contraction or artifact, for approximation and detail coefficients, respectively. A high value for the sample buffer length could result in a prohibitively large history buffer. At each level of the DWT, however, the data rate is halved, so it is possible to store a longer history with fewer samples while retaining the general trend of the signal. Furthermore, in a hardware implementation, this reduces the area overhead, delay, and power consumption for computing the local threshold. The second and third parameters affect the probability that the algorithm will attribute pressure increases to actual bladder contractions or artifacts, and they can be individually adjusted to achieve the desired performance.

We defined three quantifiable metrics from the output of the algorithm: 1) the success or failure of event detection (X), effectively the true positive rate; 2) the number of false positives detected per contraction event (Y), and the duty cycle of the stimulator, which measures the time the stimulator is on divided by the total duration of the recording (Z). Together, these metrics aggregate the effectiveness of the algorithm at detecting an unwanted bladder event with sufficiently short delay to prevent the unwanted event with electrical stimulation. We defined a cost function termed the Conditional Stimulation Score (CS Score) that combines these three metrics to tune the algorithm and to compare performance to other algorithms:

$$CS\_Score(x,y,z) = x^2 - \left(\frac{y}{100} + \frac{|z|}{10}\right) \tag{3}$$

$$x = \frac{\text{Events Detected}}{\text{Total Events}} \tag{4}$$

$$y = \frac{\text{False Positives}}{1 + \text{Events Detected}} \tag{5}$$

$$z = \frac{DC_{\text{actual}} - DC_{\text{ideal}}}{DC_{\text{ideal}}} \tag{6}$$

$$DC_{\text{actual}} = \frac{T_{\text{stim}_{\text{on}}}}{T_{\text{total}}},\ DC_{\text{ideal}} = \frac{T_{\text{contraction}}}{T_{\text{total}}}.$$

Due to the importance of a high detection rate, the percentage of true positives (x) is squared in order to penalize input

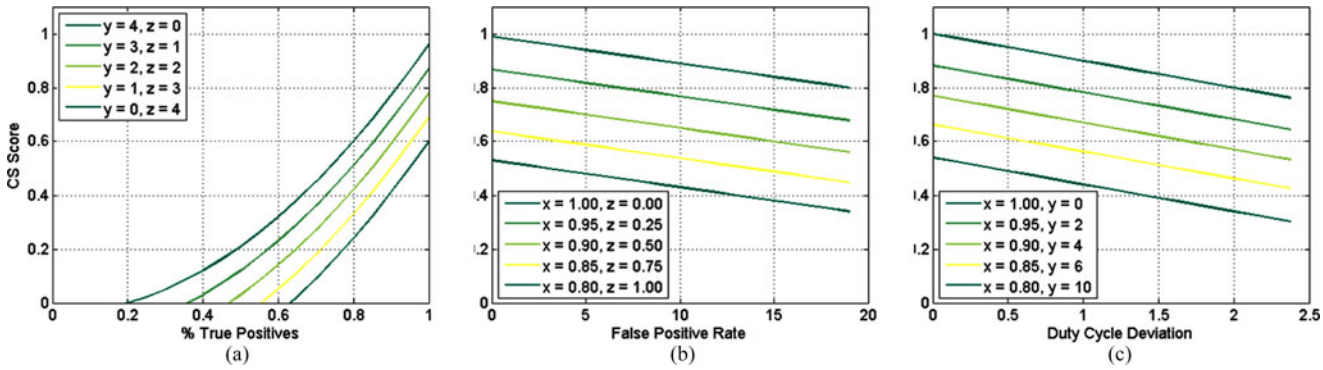

Fig. 3. (a) Quadratic term X penalizes inaccurate detection algorithms, while (b) every five false positives decrease the score by 0.05. Finally, (c) shows the penalty for oversensitivity resulting in higher duty cycle deviations, a deviation of $\pm 50\%$ also reduces the score by 0.05.

TABLE I
SUMMARY OF THE SIX ALGORITHMS TESTED

Type	Name	Abb.	Tuned?	Inputs	Description
Static	Static Detrusor Thresholding [25]	SDT	No	0	Static threshold on P_{det}
	Global Detrusor Thresholding	GDT	Yes	1	Static threshold on P_{det}
	Global Vesical Thresholding	GVT	Yes	1	Static threshold on P_{ves}
Hybrid	Hybrid Detrusor Thresholding [22]	HDT	No	0	Moving average + static threshold on P_{det}
Adaptive	Adaptive Vesical Thresholding	AVT	Yes	2	Moving threshold on P_{ves}
	Context Aware Thresholding	CAT	Yes	3	Moving threshold on approximation of P_{ves}

parameters resulting in a value below 1, while perfect detection remains unchanged. False positives (y) and duty cycle deviation (z) are linear terms weighted such that every five false positives, and every $\pm 50\%$ deviation from the ideal duty cycle result in an equivalent decrease in CS Score. Additionally, combining these terms allows the system to compensate for either 1) a high number of short duration false positives (i.e., high y, low z), or 2) a small number of high duration false positives (i.e., low y, high z), which result in scoring penalties regardless.

Example CS Scores for various parameter combinations are shown in Fig. 3. Algorithms may have the potential for a significant number of false positives, especially with noisy or real-world data, and so values ranging from 0 to 20 have been chosen to demonstrate the effect that a high number of false positives will have on the algorithm score.

C. Human Data Acquisition

Urodynamic examinations providing vesical and abdominal pressure data were collected from a total of 64 tracings from 14 human subjects sampled at 100 Hz. Note that these data were not collected for the purpose of developing this algorithm, and the sampling rate was chosen or set by the clinical equipment for the particular needs. Subjects had neurogenic detrusor overactivity and two to nine cystometric fills were completed. These clinical tests were conducted at the Louis Stokes Cleveland Department of Veterans Affairs in Cleveland, OH (IRB #12023-H12). All procedures followed protocols that were reviewed and approved by the Institutional Review Board and followed standard clinical practices.

Pressures were recorded as part of clinically standard urodynamics test, which involves filling the bladder with saline to observe its behavior [29]. Briefly, a dual lumen intraurethral catheter was inserted, with one lumen used to infuse saline into the bladder at approximately 50 ml/min, depending on the clinical scenario, and the other lumen used to measure continuous vesical pressure via an external fluidic transducer. In addition, an anorectal balloon catheter was inserted to similarly measure continuous abdominal pressure; continuous detrusor pressure was calculated as the difference between the vesical and rectal pressures. Filling was continued until a reflex bladder contraction was evoked, which usually resulted in voiding around the urethral catheter. After each cystometric fill, the bladder was completely emptied.

D. Algorithm Evaluation

To evaluate the efficacy of the CAT algorithm classifying bladder contractions and to compare to other methods, we implemented the algorithms in MATLAB (Mathworks, Natick, MA) and tested them with the recorded urodynamics data from human subjects. A summary of the algorithms tested is provided in Table I. Three other methods besides those from the literature (SDT and HDT), and the proposed method (CAT), are also included for comparison purposes. Global detrusor thresholding (GDT) and global vesical thresholding (GVT), which are derived from SDT, are used to demonstrate how a static thresholding method may be viable on either detrusor (GDT) or vesical (GVT) pressures if the threshold is tuned to an individual. Adaptive vesical thresholding (AVT), which is a variant of CAT, does not include an intermediate DWT and is used to demonstrate the effect of performing thresholding on the wavelet coefficients rather than the time domain signal.

During testing, a real-time environment was simulated in which the algorithms were limited to accessing data on the time course in which it was produced, without access to future

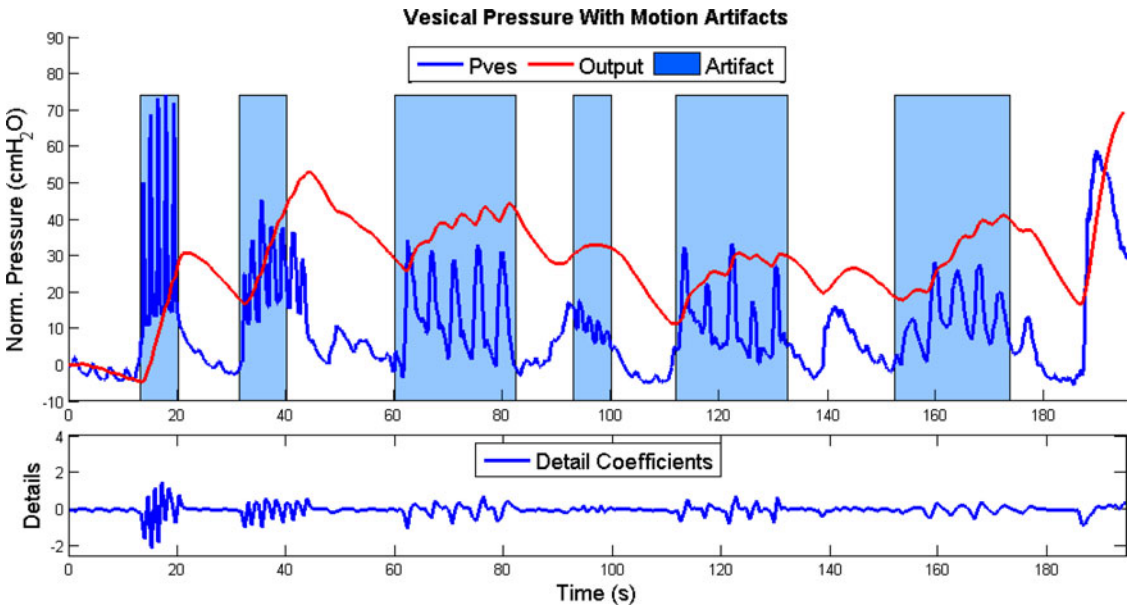

Fig. 4. Original vesical pressure (blue) and final output (red), showing the location of an artifact (blue shading). Below, detail coefficients demonstrating real-time detection of artifacts. 1) cough, 2) laugh, 3) vertical press, 4) hum, 5) bend over in chair, and 6) raise object from lap.

data. Then, for each algorithm, the CS Score was calculated to compare their performances. Algorithms were tuned using two methods. First, they were tuned to each individual using only the first of the available urodynamics tracings; parameters generated from each training set were applied to the same individual. Second, algorithms were tuned to a subset of 14 tracings, one from each patient, and applied to the entire dataset.

For both training methods, the onset of a contraction was identified by inspection. Each recorded cystometric fill contained exactly one voiding contraction; thus, any events detected outside of this range were considered to be false positives. To effectively inhibit an unwanted contraction, stimulation must occur well before the leak point pressure is reached; therefore, we assumed contractions must be detected within 1 s for effective stimulation, and any events detected after this time were considered missed events.

E. Algorithm Tuning

While SDT and HDT were implemented as described in the literature, the other methods were tuned to individuals by modifying parameters to maximize the CS Score for that algorithm. These parameters include the low-pass filter cutoff frequency (for all tuned algorithms), as well as algorithm-specific parameters: static threshold (GDT and GVT), history buffer length (AVT and CAT), sensitivity (AVT), and approximation/detail sensitivities (CAT). Thresholds between -50 and 50 $\mathrm{cmH_2O}$ were tested for GDT and GVT. Windows ranging from 5 to 120 s were tested for both AVT and CAT. Sensitivities between 0 and 1 were tested for AVT sensitivity and both approximation and detail coefficients for CAT. These parameters were found to have a significant impact on the performance of each algorithm, with per-subject detection accuracies ranging from 0% to 100%, false positive rates ranging from none to hundreds, and CS Scores ranging from negative tens to nearly perfect scores. The algorithm was considered tuned when a parameter combination resulting in the largest CS Score was found. Similarly, a global tuning method was explored, where parameters were tuned based on a subset of the data and applied to the remainder. Here, a more robust algorithm would still perform well, though not as well as with individualized tuning.

In practice, the sudden and repeated application of conditional stimulation could cause patient discomfort, so parameter optimization must seek to 1) maximize detection accuracy, 2) minimize false positives, 3) minimize detection latency between contraction onset and event detection, and 4) minimize the stimulator duty cycle. Failure to select appropriate parameters can result in oversensitivity to noise or other low amplitude pressure fluctuations. With optimally chosen parameters, a reliable and robust algorithm will have consistently high detection rates while similarly limiting the number of false positives.

Resulting CS Scores were analyzed using Tukey's pairwise comparison ($p < 0.05$) to determine if CAT is more effective than the other methods for detecting bladder contractions. Data from tuned methods and untuned methods were pooled to determine if tuning can improve efficacy. Finally, data from static methods (GDT, GVT) and adaptive methods (AVT, CAT) were pooled and tested to determine if adaptive methods are more effective than the static methods.

III. Results

In this section, we present results for CAT and provide comparisons to the other algorithms tested.

A. Context Aware Thresholding

Bladder pressure is a smooth signal relative to pressures caused by abdominal pressures, and slopes in an appropriately sized window can be approximated well with linear functions. Most artifacts due to abdominal pressure changes, such as those

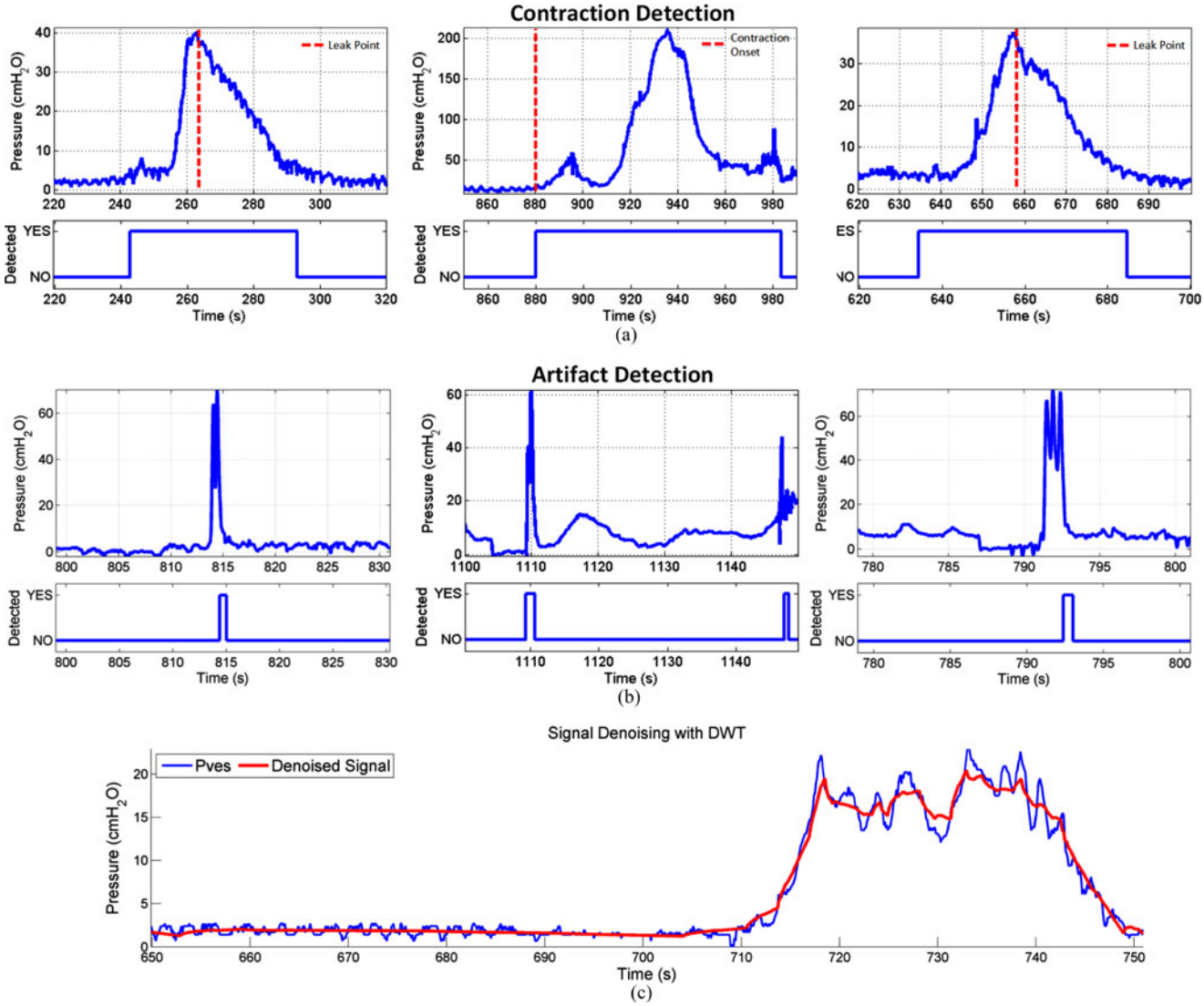

Fig. 5. Sample outputs of the CAT algorithm. Rapid categorization of (a) bladder events and (b) artifacts. (c) DWT for denoising applications in blue, the original noisy vesical pressure signal; in red, the reconstructed, denoised signal.

initiated by coughs, laughs, and sneezes, generally present as abrupt, transient spikes in the vesical pressure and thus appear in the detail coefficients, as shown in Fig. 4, where they were analyzed as potential artifacts. While simple changes in posture could have an effect on the vesical pressure, these types of slowly changing pressure artifacts were not tested in this study because they were not reliably present in the data set.

Fig. 5 shows sample outputs from the CAT algorithm, specifically contraction detection (a) well before the contraction onset or leak point pressure (dashed line) and artifact detection (b), which were not classified as contractions due to the higher rate of pressure increase. Finally, Fig. 5(c) gives an example of the denoising capabilities of wavelets, which demonstrates how adaptive thresholding in the wavelet domain can improve the specificity of the detection algorithm.

B. Algorithm Comparisons

Three static methods (SDT, GDT, GVT) were tested using different threshold values. With SDT, the same threshold of 10 cmH_2O was used for each urodynamic tracing, while GDT and GVT were both tuned to individuals. Similarly, three adaptive methods (HDT, AVT, CAT) were tested. Algorithms were compared, testing the contraction detection rate, false positive rate, duty cycle deviation, and overall CS Score (see Fig. 6). Results for both individualized and global tuning are summarized in Tables II and III.

TABLE II
SUMMARY OF RESULTS FOR INDIVIDUALIZED TUNING (STANDARD DEVIATION SHOWN)

Type	Method	True Pos. (%)	False Pos.	Score
Static	SDT	0.76 ± 0.2	21.6 ± 22.5	-0.19 ± 0.8
	GDT	0.70 ± 0.2	0.6 ± 0.5	0.50 ± 0.2
	GVT	0.74 ± 0.3	0.4 ± 0.3	0.56 ± 0.2
Hybrid	HDT	0.75 ± 0.3	18.6 ± 15.9	-0.03 ± 0.8
Adaptive	AVT	0.85 ± 0.1	1.4 ± 1.3	0.78 ± 0.1
	CAT	0.97 ± 0.1	1.3 ± 1.0	0.82 ± 0.1

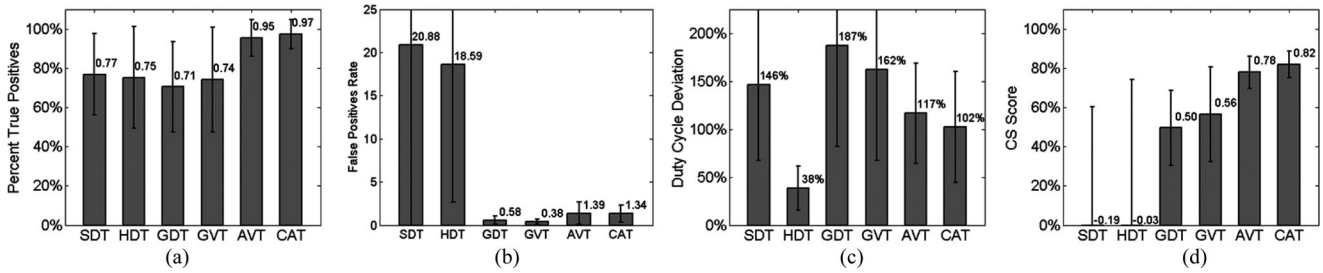

Fig. 6. Three derived metrics [accuracy (a), false positive rate (b), and duty cycle deviation (c)], and resulting CS Scores (d) for all algorithms tested.

TABLE III
SUMMARY OF RESULTS WITH GLOBAL TUNING
(STANDARD DEVIATION SHOWN)

Type	Method	True Pos. (%)	False Pos (%)	Score
Static	SDT	0.76 ± 0.2	21.6 ± 22.5	-0.19 ± 0.8
	GDT	0.88 ± 0.3	2.26 ± 2.4	0.54 ± 0.3
	GVT	0.90 ± 0.3	2.04 ± 2.4	0.51 ± 0.3
Hybrid	HDT	0.75 ± 0.3	18.6 ± 15.9	-0.03 ± 0.8
Adaptive	AVT	0.84 ± 0.4	8.10 ± 7.9	0.65 ± 0.3
	CAT	0.96 ± 0.2	9.24 ± 7.3	0.75 ± 0.2

As a hybrid of static and adaptive methods, HDT did not perform significantly better than either of the static methods, despite having a moving threshold. Conversely, AVT and CAT both demonstrated significant improvements in detection accuracy (95% and 97%, respectively) over static methods, though the false positive rates increased slightly when compared with GDT and GVT. For most tracings, operating in the wavelet domain resulted in fewer false positives while maintaining a high degree of accuracy.

From a latency perspective, the CS Score accounts only for whether or not detection occurred within 1 s of contraction; the precise latency is not used for scoring. Therefore, it is important to note the differences in detection latency between the algorithms, as shown in Fig. 7 for a subset of detections. Note that negative latencies represent detection prior to contraction onset. CAT is more likely to detect contraction onset a short time in advance, reducing the possibility of overstimulation.

Using Tukey's pairwise comparisons, we found that a significant difference existed between the two methods not tuned to individuals (SDT, HDT) and the four that were (GDT, GVT, AVT, and CAT). Among tuned methods, we found a significant difference existed between the two purely static methods (GDT, GVT) and the purely adaptive methods (AVT, CAT). From this, we concluded that tuning the algorithm to an individual can improve performance even for a static method. Compared with AVT, the addition of the DWT improves CAT by providing two signal outputs for event detection, reducing the occurrence of false positives, and allowing for more efficient hardware implementation.

IV. DISCUSSION

There is a small time window during which stimulation will be effective at inhibiting bladder contractions once the contraction has begun. The leak point pressure, the point at which the pressure has sufficiently risen to cause a leak, can often take several seconds to reach after the onset of contraction. However, stimulation must begin well before this pressure is reached. We accounted for stimulation onset delay and transmission latency by assuming that the system must detect an event within 1 s of contraction onset to successfully prevent a leak. Given this constraint, it was necessary to find a level of signal decomposition that met the delay requirement while yielding the best possible approximation. We found that a fifth-level decomposition, when paired with an initial EMA filter, improved the output result and offered an acceptable balance between the decay rate of artifacts and attenuation of other high frequency noise sources, without violating the delay requirements.

Note that in a closed-loop neuromodulator, bladder pressure will decrease when contractions are averted by stimulation; as such, the concept of duty cycle only makes sense on a recording used for tuning purposes. Nevertheless, it is important to consider this metric because an ideally tuned algorithm should only begin detecting the contraction at contraction onset and end detection when the contraction has subsided. Therefore, the closer the stimulation duty cycle is to that of the contraction, the more attuned the algorithm is to the individual tracing. In practice, a more important metric is the detection latency, which is reported in the results due to its real-world applicability.

A. Detection Accuracy and False Positives

In addition to the scoring system, rates of accuracy and false positives must also be viewed in a clinical context. Patients suffering from OAB can typically expect to experience eight or more contractions within a 24-h period [2]. The false positive rates measured in our experiments are reported as the number of false positives per contraction event; therefore, an adaptive thresholding technique like CAT could result in ten extra stimulations per day. This would be a significant improvement over open-loop continuous stimulation, which drains the power supply, while potentially habituating the patient to a certain level of stimulation. Comparatively, tuned static thresholds like GDT or GVT could result in 7–14 stimulations per day. However, the contraction detection rate is approximately 73%, so these methods may provide inferior contraction prevention. The use of untuned static or adaptive methods could result in several hundred unnecessary stimulations per day, especially if the sensor output becomes noisy or drifts, or if patient behavior leads to a large number of abdominal pressure artifacts.

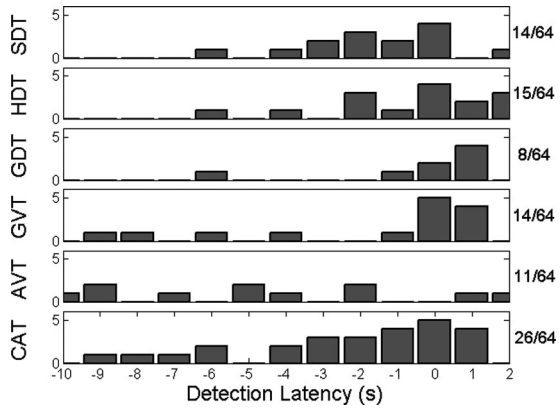

Fig. 7. Detection latencies for each of the six algorithms, specifically those for which detection occurs within the interval [−10,1] s from contraction onset. Shown on the right are the number of samples falling in this range.

B. Detection of Artifacts

For an automated bladder event detection system, detecting every artifact event may not be desirable, since it may be beneficial to stimulate on certain noncontraction events. For some patients, especially those with SUI, certain triggers that would normally be considered artifacts, such as laughs or coughs, may instigate urine leakage [30]. Activities such as bending over result in sustained rises in pressure and can mimic bladder contractions such that the system will suggest stimulation despite a lack of bladder activity. The need to minimize false positives is therefore something a patient might influence, e.g., in nonsensate patients, the algorithm can be tuned to increase sensitivity to such events. The false positive rate will increase, but at the request of and in the best interests of the patient.

In our study, the input parameters were varied to fine tune each algorithm to a single patient. From the SDT, GDT, and GVT results, we observed that a simple threshold is ineffective for controlling a conditional stimulator, given the large intra- and interpatient threshold variation. Similarly, the computation of the moving threshold of HDT is relatively simple, but the constant threshold of 5 cmH_2O resulted in a significant number of false positives, especially for noisy data. Conversely, the adaptive methods AVT and CAT both demonstrated significant improvements when considering both detection rate and false positives, at the cost of increased computational complexity. For individual tuning, CAT detected 97% of contractions within 1 s of onset without a significant number of false positives. For global tuning, the detection accuracy decreased slightly, and the false positive rate increased, but the CS Score was still greater than the other algorithms, making it the best choice for analysis of multiple urodynamics tracings and constant recordings from one patient, as well as a conditional stimulation trigger.

C. Hardware Implementation

The CAT algorithm was designed to balance performance with the cost of hardware implementation. The initial filtering contains only one delay unit, and requires one multiplication and two signed additions. The lifting scheme [31], [32] is commonly used for hardware implementations of the DWT, and previous work [33] has demonstrated energy-efficient design techniques, leading to a 20-channel DWT-based digital signal processor for implantable neural microsystems synthesized in 70-nm technology with an area of just 0.21 mm^2 consuming 10 μW of power. While adaptive thresholding is more complex to implement in hardware, its performance over global static thresholding warrants the extra cost. In addition, the buffer is constantly partially sorted, and only one new sample must be ranked for each iteration. This insertion type is a relatively inexpensive operation for which efficient hardware implementations already exist [34].

D. Stimulation Routines

By itself, the CAT algorithm is not designed to directly control a stimulator. Rather, it enables real-time detection and categorization of specific bladder events and is capable of distinguishing them from artifacts, useful for a closed-loop stimulation system. A conventional continuous stimulator, such as the Medtronic Interstim [11], can potentially be integrated with an event-detection system that implements the proposed algorithm. Categorizing events rather than directly controlling stimulation provides the necessary flexibility to aid in diagnosis and treatment of a wide range of lower urinary tract disorders. Though this study focused on detecting voiding contractions, detection of nonvoiding contractions is possible with the same system. These events are generally shorter in duration and intensity, and have different pressure rise and fall times compared to voiding contractions. Stimulating on voiding contractions can be desirable if the patient has neurogenic bladder, as the contractions are not controlled by the individual. However, different patients will likely require different stimulation routines or patterns for various bladder events.

V. Conclusion

In this study, we have presented CAT, a real-time highly accurate bladder event detection system that does not require an abdominal reference sensor. Compared with static methods, CAT offers consistently accurate classification with few false positives and can therefore be used to augment existing diagnostic and treatment techniques for urinary incontinence, including ambulatory urodynamics and closed-loop neuromodulation. The presented patient-specific optimization method improves accuracy for both static and adaptive algorithms; the tunable parameters can be adjusted to increase noise tolerance, reduce false positives, or increase sensitivity, achieving the desired balance between patient comfort and treatment efficacy. The algorithm was designed to be efficient in hardware, and future work will focus on this implementation, as well as its clinical evaluation and use with wireless implantable bladder pressure sensors for providing closed-loop feedback to a commercial stimulator. Finally, applications to computer-aided diagnostics of lower urinary tract dysfunction will also be investigated.

References

[1] R. Voelker, “International group seeks to dispel incontinence ‘taboo’,” *JAMA: J. Am. Med. Assoc.*, vol. 280, no. 11, pp. 951–953, 1998.

[2] E. Gormley *et al.*, "Diagnosis and treatment of overactive bladder (non-neurogenic) in adults: AUA/SUFU guideline," *J. Urol.*, vol. 188, no. 6, pp. 2455–2463, 2012.
[3] D. Gould *et al.*, "The effect of posture on bladder pressure," *J. Physiol.*, vol. 129, no. 3, pp. 448–453, 1955.
[4] E. V. W. Van Doom *et al.*, "Extramural ambulatory urodynamic monitoring during natural filling and normal daily activities: Evaluation of one hundred patients," *J. Urol.*, vol. 146, pp. 124–131, 1991.
[5] K. L. Rademakers *et al.*, "Differentiation of lower urinary tract dysfunctions: The role of ambulatory urodynamic monitoring," *Int. J. Urol.*, vol. 22, no. 5, pp. 503–507, 2015.
[6] J. Wheeler, Jr, *et al.*, "Bladder inhibition by penile nerve stimulation in spinal cord injury patients," *J. Urol.*, vol. 147, no. 1, pp. 100–103, 1992.
[7] Y.-H. Lee and G. H. Creasey, "Self-controlled dorsal penile nerve stimulation to inhibit bladder hyperreflexia in incomplete spinal cord injury: A case report," *Arch. Phys. Med. Rehabil.*, vol. 83, no. 2, pp. 273–277, 2002.
[8] A. Dalmose *et al.*, "Conditional stimulatzion of the dorsal penile/clitoral nerve may increase cystometric capacity in patients with spinal cord injury," *Neurourol. Urodynamics*, vol. 22, no. 2, pp. 130–137, 2003.
[9] F. Martens *et al.*, "Minimal invasive electrode implantation for conditional stimulation of the dorsal genital nerve in neurogenic detrusor overactivity," *Spinal Cord*, vol. 49, no. 4, pp. 566–572, 2010.
[10] H. B. Goldman *et al.*, "Dorsal genital nerve stimulation for the treatment of overactive bladder symptoms," *Neurourol. Urodynamics*, vol. 27, no. 6, pp. 499–503, 2008.
[11] Sacral neuromodulation. Online. (2015). [Online]. Available: http://professional.medtronic.com/pt/uro/snm/index.htm
[12] A. Kirkham *et al.*, "The acute effects of continuous and conditional neuromodulation on the bladder in spinal cord injury," *Spinal Cord*, vol. 39, no. 8, pp. 420–428, 2001.
[13] S. Jezernik *et al.*, "Detection and inhibition of hyperreflexia-like bladder contractions in the cat by sacral nerve root recording and electrical stimulation," *Neurourol. Urodynamics*, vol. 20, no. 2, pp. 215–230, 2001.
[14] E. E. Horvath *et al.*, "Conditional and continuous electrical stimulation increase cystometric capacity in persons with spinal cord injury," *Neurourol. urodynamics*, vol. 29, no. 3, pp. 401–407, 2010.
[15] B. J. Wenzel *et al.*, "Detecting the onset of hyper-reflexive bladder contractions from the electrical activity of the pudendal nerve," *IEEE Trans. Neural Syst. Rehabil. Eng.*, vol. 13, no. 3, pp. 428–435, Sep. 2005.
[16] T. M. Bruns *et al.*, "Multielectrode array recordings of bladder and perineal primary afferent activity from the sacral dorsal root ganglia," *J. Neural Eng.*, vol. 8, no. 5, p. 056010, 2011.
[17] A. Mendez *et al.*, "Estimation of bladder volume from afferent neural activity," *IEEE Trans. Neural Syst. Rehabil. Eng.*, vol. 21, no. 5, pp. 704–715, Sep. 2013.
[18] J. Coosemans and R. Puers, "An autonomous bladder pressure monitoring system," *Sens. Actuators A, Phys.*, vol. 123, pp. 155–161, 2005.
[19] C.-C. Wang *et al.*, "A mini-invasive long-term bladder urine pressure measurement ASIC and system," *IEEE Trans. Biomed. Circuits Syst*, vol. 2, no. 1, pp. 44–49, Mar. 2008.
[20] F. Axisa *et al.*, "Design and fabrication of a low cost implantable bladder pressure monitor," in *Proc. Annu. Int. Conf. IEEE Eng. Med. Biol. Soc.*, 2009, pp. 4864–4867.
[21] P. Jourand and R. Puers, "The bladderpill: An in-body system logging bladder pressure," *Sens. Actuators A, Phys.*, vol. 162, no. 2, pp. 160–166, 2010.
[22] J. Melgaard and N. Rijkhoff, "Detecting the onset of urinary bladder contractions using an implantable pressure sensor," *IEEE Trans. Neural Syst. Rehabil. Eng.*, vol. 19, no. 6, pp. 700–708, Dec. 2011.
[23] S. Majerus *et al.*, "Low-power wireless micromanometer system for acute and chronic bladder-pressure monitoring," *IEEE Trans. Biomed. Eng.*, vol. 58, no. 3, pp. 763–767, Mar. 2011.
[24] S. J. Majerus *et al.*, "Wireless, ultra-low-power implantable sensor for chronic bladder pressure monitoring," *ACM J. Emerging Technol. Comput. Syst.*, vol. 8, no. 2, p. 11, 2012.
[25] J. Hansen *et al.*, "Treatment of neurogenic detrusor overactivity in spinal cord injured patients by conditional electrical stimulation," *J. Urol.*, vol. 173, no. 6, pp. 2035–2039, 2005.
[26] J. Melgaard *et al.*, "Detecting urinary bladder contractions: Methods and devices," *J. Sens. Technol.*, vol. 4, no. 04, p. 165, 2014.
[27] C. C. Holt, "Forecasting seasonals and trends by exponentially weighted moving averages," *Int. J. Forecasting*, vol. 20, no. 1, pp. 5–10, 2004.
[28] I. Daubechies *et al.*, *Ten Lectures on Wavelets*, vol. 61. Philadelphia, PA, USA: SIAM, 1992.
[29] J. Previnaire *et al.*, "Long-term effect of prudendal nerve electrical stimulation on detrusor hyper-reflexia in spinal cord injury patients," *Ann. Readaptation et de Med. Phys.*, vol. 39, no. 5, pp. 297–300, 1996.
[30] I. E. Nygaard and M. Heit, "Stress urinary incontinence," *Obstetrics Gynecol.*, vol. 104, no. 3, pp. 607–620, 2004.
[31] W. Sweldens, "The lifting scheme: A construction of second generation wavelets," *SIAM J. Math. Anal.*, vol. 29, no. 2, pp. 511–546, 1998.
[32] I. Daubechies and W. Sweldens, "Factoring wavelet transforms into lifting steps," *J. Fourier Anal. Appl.*, vol. 4, no. 3, pp. 247–269, 1998.
[33] S. Narasimhan *et al.*, "Ultra-low-power and robust digital-signal-processing hardware for implantable neural interface microsystems," *IEEE Trans. Biomed. Circuits Syst.*, vol. 5, no. 2, pp. 169–178, Apr. 2011.
[34] C. Chakrabarti, "Sorting network based architectures for median filters," *IEEE Trans. Circuits Syst. II, Analog Digital Signal Process.*, vol. 40, no. 11, pp. 723–727, Nov. 1993.

Authors' photographs and biographies not available at the time of publication.